Chapter 7

REMOVAL OF CADMIUM USING NANO CRYSTALLINE ZIRCONIA

In this chapter, the capability of synthesized nano crystalline zirconia is assessed for removal of cadmium from aqueous solutions. In addition to this, effect of various parameters and their significance in cadmium removal from aqueous solutions has been explained. The isotherm and kinetic parameter determination by linear and nonlinear equations are also assessed. Thermodynamic parameters were determined for better understanding of the feasibility and nature of the removal process.

7.1. Adsorption experiments

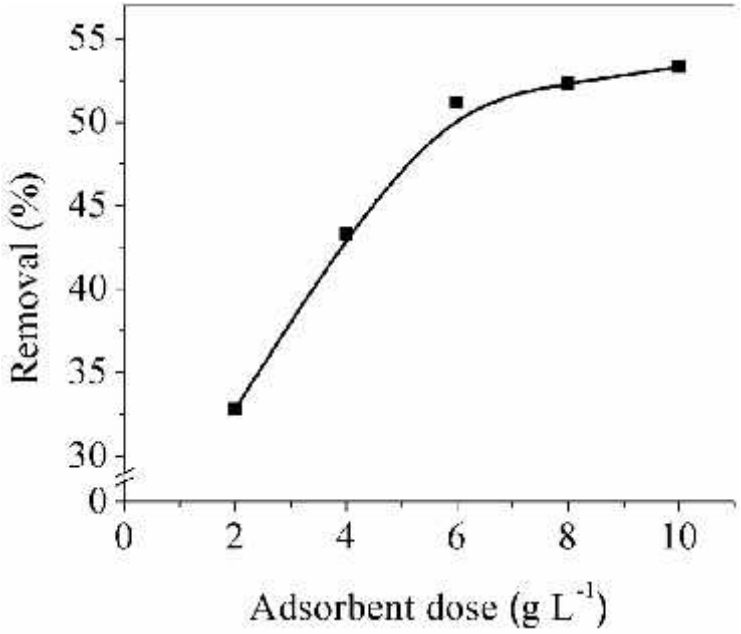

Figure 7.1 Effect of adsorbent dose on removal (%) of cadmium from aqueous solutions on nano crystalline zirconia (Initial pH=7, Initial concentration 10 mg L^{-1}, Temperature 303K)

Preliminary studies were conducted removal of cadmium from aqueous solutions. Effect of pH is studied by varying initial pH from 2 to 7 (Figure 7.2). The cadmium removal (%) was nil at pH 2 and increased on raising initial pH. The effect of adsorbent dose is studied by varying adsorbent dose from 2g L^{-1} to 10 g L^{-1}. The cadmium removal increased from ca. 32% to 53 %. Similarly, the effect of initial concentration is studied by varying initial concentration from 0.5 mg L^{-1} to 50 mg L^{-1}. The cadmium removal (%) declines from 100% to 10% on increasing initial concentration from 0.5 mg L^{-1} to 50 mg L^{-1} (Figure 7.3). On the basis of aforementioned results, the initial concentration in RSM study ranged

from 1 mg L^{-1} to 10 mg L^{-1}, Initial pH from 4 to 7 and adsorbent dose from 4 g L^{-1} to 8 g L^{-1} (Figure 7.1). On studying effect of time, the equilibrium time was found to be 20 min (Figure 7.4).

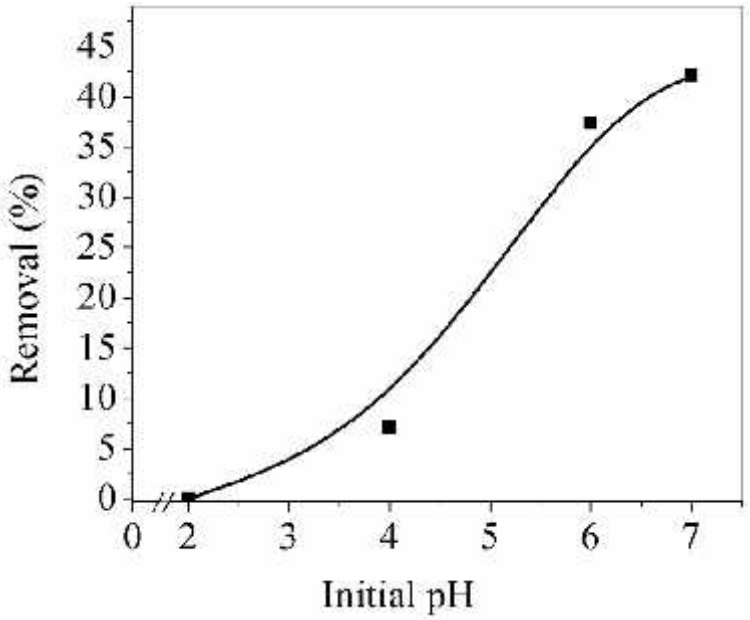

Figure 7.2 Effect of initial pH on removal (%) of cadmium from aqueous solutions on nano crystalline zirconia (Initial concentration = 10 mg L^{-1}, adsorbent dose 2 g L^{-1} Temperature= 303 K)

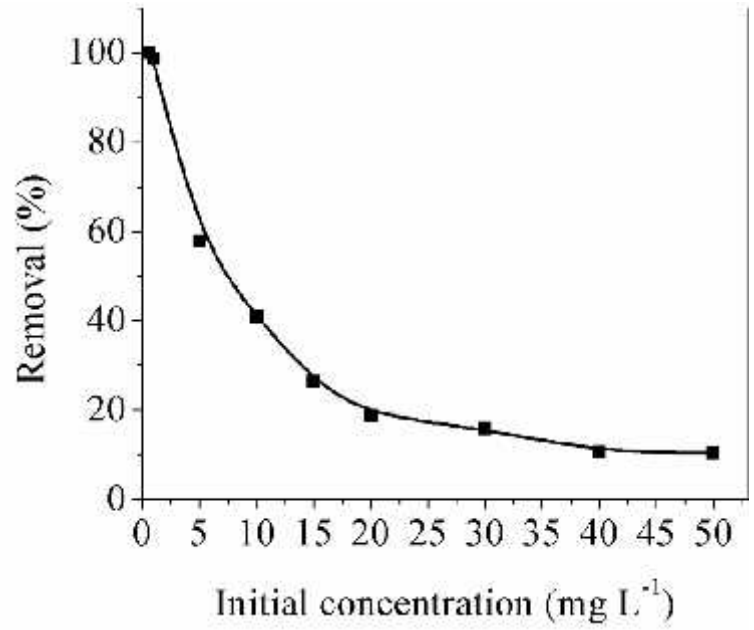

Figure 7.3 Effect of initial concentration on removal (%) of cadmium from aqueous solutions on nano crystalline zirconia (Initial pH= 7, adsorbent dose 2g L^{-1}, Temperature 303 K)

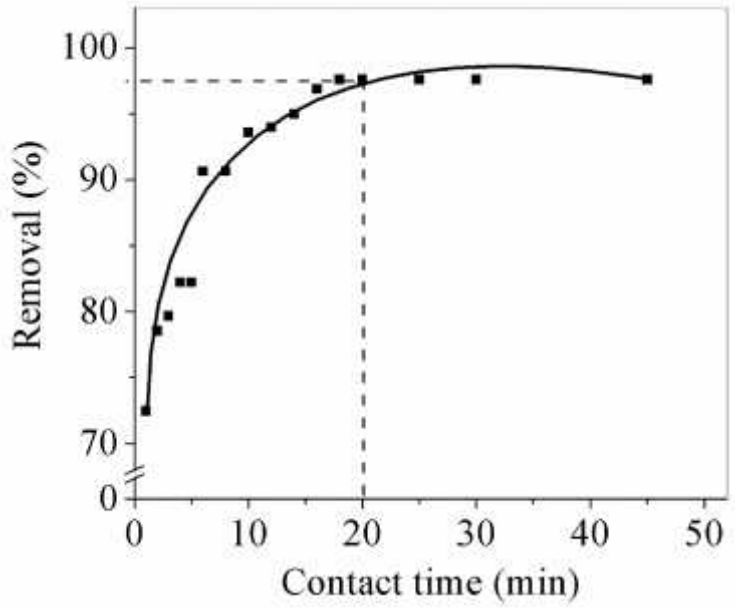

Figure 7.4 Effect of contact time on removal (%) of cadmium from aqueous solutions on nano crystalline zirconia (Initial concentration 1 mg L^{-1}, Initial pH =7, adsorbent dose 2 g L^{-1}, Temperature= 303 K)

7.1.1. Data analysis and construction of regression model

Regression analysis equation in coded terms of the experimental data for the removal (%) of cadmium is represented by the following regression equation:

Y = 50.65 - 13.79 (initial concentration) + 28.998 (pH) + 3.3653 (adsorbent dose) + 2.3753 (initial concentration)^2 + 2.2484 (pH)^2 - 8.6067 (adsorbent dose)^2 - 12.3116 (initial concentration x pH) + 0.3084 (initial concentration x adsorbent dose) - 0.5966 (pH x adsorbent dose) (7.1)

The empirical model in terms of actual parameters (uncoded) is represented as follows:

Y= -153.198 + 5.47124 (Initial concentration) + 19.5648 (pH) + 28.4080 (Adsorbent dose) + 0.117299 (Initial concentration x Initial concentration) + 0.999272 (pH x pH) - 2.15167 (Adsorbent dose x Adsorbent dose) – 1.82394 (Initial concentration x pH) +0.0342694 (Initial concentration x Adsorbent dose) - 0.198858 (pH x Adsorbent dose) (7.2)

Table 7.1 Box-Behnken designed experimental runs for removal of cadmium utilizing nano crystalline zirconia

Run Order	Initial conc. (mg L^{-1})	pH	Adsorbent dose (g L^{-1})	Removal (%)
1	1	4	4	12.90
2	10	4	4	14.83
3	1	7	4	100.00
4	10	7	4	47.93
5	1	4	8	20.04
6	10	4	8	18.45
7	1	7	8	100.00
8	10	7	8	53.92
9	1	5.5	6	75.75
10	10	5.5	6	35.66
11	5.5	4	6	28.40
12	5.5	7	6	82.75
13	5.5	5.5	4	36.27
14	5.5	5.5	8	53.18
15	5.5	5.5	6	47.73
16	5.5	5.5	6	51.54
17	5.5	5.5	6	49.00
18	5.5	5.5	6	48.00
19	5.5	5.5	6	49.00
20	5.5	5.5	6	48.00

7.1.2. Regression analysis and ANOVA

In current study, regression coefficient (R^2) is 97.87% and Adjusted R^2 (R^2_{adj}) was 95.96% (Table 7.2) found to be more than 80%; it depicts good fit of the regression model. The R^2 values recommend justifiability of quadratic model for adsorption of cadmium on nano crystalline zirconia. The terms with p value more than 0.05 considered to be non significant. Initial concentration, initial pH and their interaction terms were judged to be significant on the basis of p value. The initial pH and adsorbent dose have positive sign prior to their coefficient. The positive sign prior to initial pH and adsorbent dose portray that increase in pH and

adsorbent dose guided to increased removal (%) of cadmium on nanocrystalline zirconia.

Table 7.2 Estimated Regression Coefficients for removal of cadmium using nano crystalline zirconia

Term	Coef	SE Coef	p
Constant	50.6591	1.744	0
Initial concentration	-13.7903	1.605	0
Initial pH	28.998	1.605	0
Adsorbent dose	3.3653	1.605	0.062
Initial concentration * Initial concentration	2.3753	3.06	0.456
Initial pH* Initial pH	2.2484	3.06	0.479
Adsorbent dose * Adsorbent dose	-8.6067	3.06	0.018
Initial concentration* Initial pH	-12.3116	1.794	0
Initial concentration * Adsorbent dose	0.3084	1.794	0.867
pH*Adsorbent dose	-0.5966	1.794	0.746
S = 5.07405 , PRESS = 1875.84			
R-Sq = 97.87% , R-Sq(pred) = 84.52% , R-Sq(adj) = 95.96%			

Table 7.3 Analysis of Variance for removal of cadmium utilizing nano crystalline zirconia

Source	**DF**	**Seq SS**	**Adj SS**	**Adj MS**	**F**	**p**
Regression	9	11857.2	11857.2	1317.46	51.17	0
Linear	3	10423.8	10423.8	3474.6	134.96	0
Initial concentration	1	1901.7	1901.7	1901.71	73.86	0
Initial pH	1	8408.8	8408.8	8408.85	326.61	0
Adsorbent dose	1	113.3	113.3	113.26	4.4	0.062
Square	3	217.1	217.1	72.38	2.81	0.094
Initial concentration* Initial concentration	1	10.4	15.5	15.52	0.6	0.456
Initial pH*Initial pH	1	3.1	13.9	13.9	0.54	0.479
Adsorbent dose*Adsorbent dose	1	203.7	203.7	203.71	7.91	0.018
Interaction	3	1216.2	1216.2	405.4	15.75	0
Initial concentration*Initial pH	1	1212.6	1212.6	1212.6	47.1	0
Initial concentration *Adsorbent dose	1	0.8	0.8	0.76	0.03	0.867
Initial pH*Adsorbent dose	1	2.8	2.8	2.85	0.11	0.746
Residual Error	10	257.5	257.5	25.75		
Lack-of-Fit	5	247.5	247.5	49.5	24.82	0.002
Pure Error	5	10	10	1.99		
Total	19	12114.6				

The magnitude of the coefficient depicts strength of the variable. The initial pH was most dominant variable followed by initial concentration and adsorbent dose. ANOVA results (Table 7.3) suggested the same results as by regression model. The initial pH was most influential variable advocated by highest sequential sum of squares (8408.8) and followed by initial concentration (1901.7) and adsorbent dose (113.3).

7.1.3. Effect of pH

Initial pH was the most dominating factor, affecting the adsorption of cadmium. In the present study, the consequence can be evidenced by Experimental run '1;3' and '2;4' (Table 7.1). The cadmium removal (%) boosts from 12.9 to 100 % with rise of pH from 4 to 7 at 1 mg L^{-1} initial concentration and adsorbent dose of 4 g L^{-1} (Experimental run 1 and 3 in Table 7.1). The decline in the pH of the solution elevates positive charge on the surface of adsorbent. Hence, electrostatic charge on the surface declined between adsorbate and adsorbent. In addition to the above mentioned electrostatic phenomenon, H^+ ions compete with the cadmium ions for adsorption on the adsorbent surface (Wang *et al.* 2010). At lower pH, there was high concentration of H^+ ions, leading to reduced uptake of cadmium.

The effect of pH on adsorption is also explained on the basis of pH_{zpc}. The pH_{zpc} of the adsorbent is 6.78. The surface of the adsorbent becomes more positive below the pH_{zpc} of the adsorbent and negative above the pH_{zpc} value. Hence, at pH below 6.78 the uptake of cadmium declines due to positive charge on the surface of adsorbent. The pH of the solution, when raised above 6.78; solution becomes negatively charge and led to increase in adsorption of cadmium.

7.1.4. Effect of adsorbent dose

The sum of squares value for adsorbent dose was least (113.3), it depicts that adsorbent was less influencing factor as compared to pH and initial concentration. There was only modest change in the cadmium removal (%) on changing adsorbent dose (Experimental runs '1;5' and '2;6' in Table 7.1). The cadmium removal (%) increased with increase of adsorbent dose or *vice versa*. The increase in adsorption of cadmium with dose was due to larger availability of number of

adsorption sites. The maximum cadmium removal (%) was achieved at 4 gL^{-1} adsorbent dose (initial concentration 1 mg L^{-1} at Experimental run 3 in Table 7.1).

7.1.5. Effect of initial concentration

Initial concentration was the penultimate dominating factor after pH. There were limited active sites on the surface of the adsorbent. The maximum cadmium removal (%) was achieved at 1 mg L^{-1} initial concentration (Experimental run 3 in Table 7.1). The increase of initial concentration to 10 mg L^{-1} (Experimental run 4 in Table 7.1) led to decline in cadmium removal from 100 % to 47.93 %. The numbers of active sites were few at higher initial concentration in comparison to adsorbate species than at lower initial concentration. So, the cadmium removal (%) is elevated on decreasing initial concentration.

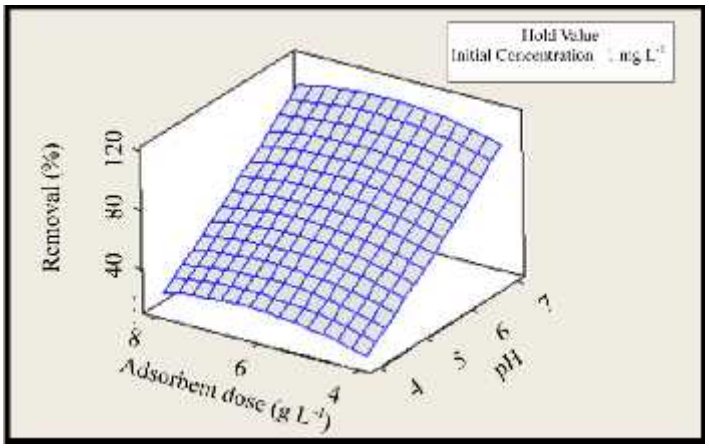

Figure 7.5 Surface plot of 'cadmium removal (%) *vs.* pH and adsorbent dose (g L^{-1})' at hold value of initial concentration at1mg L^{-1}

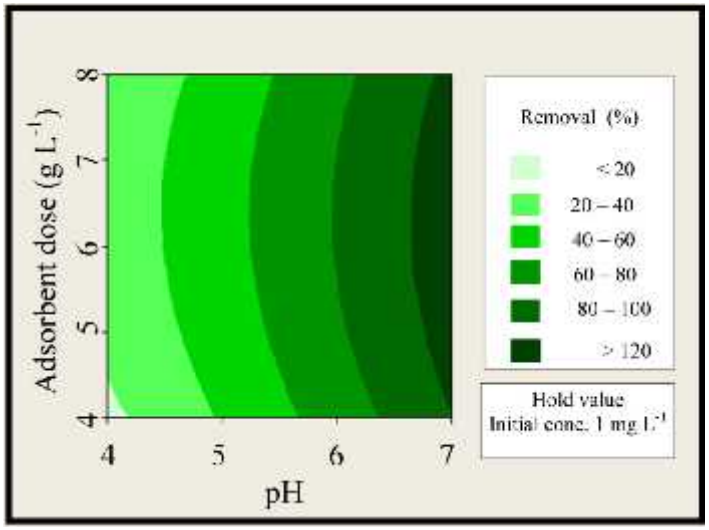

Figure 7.6 Contour plot of 'cadmium removal (%) *vs.* pH and adsorbent dose (g L^{-1})' at hold value of initial concentration at 1 mg L^{-1}

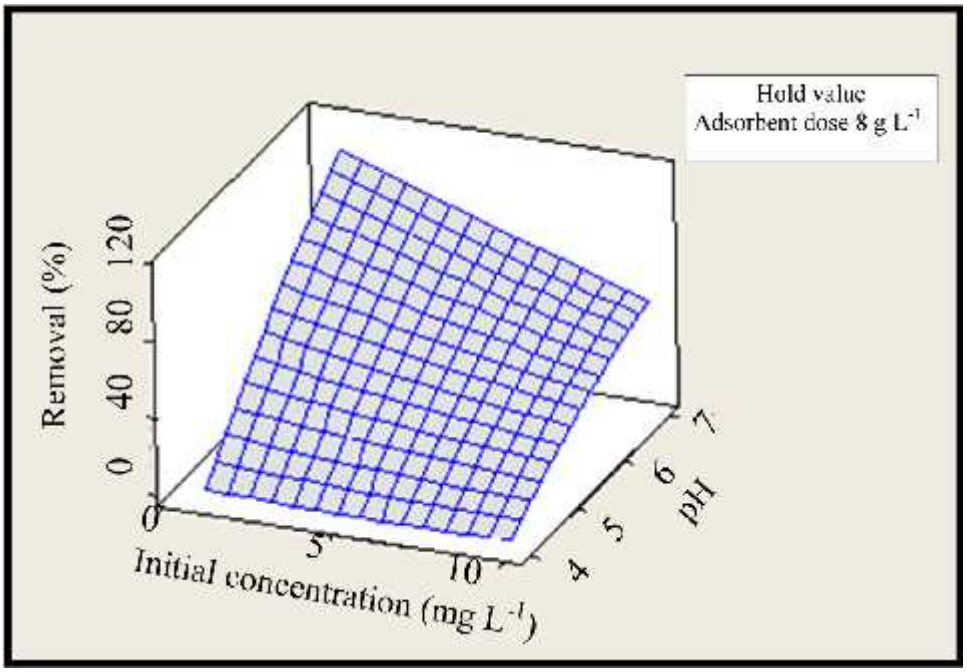

Figure 7.7 Surface plot of 'cadmium removal (%) *vs.* pH and initial concentration (mg L^{-1})' at hold value of adsorbent dose at 8 g L^{-1}

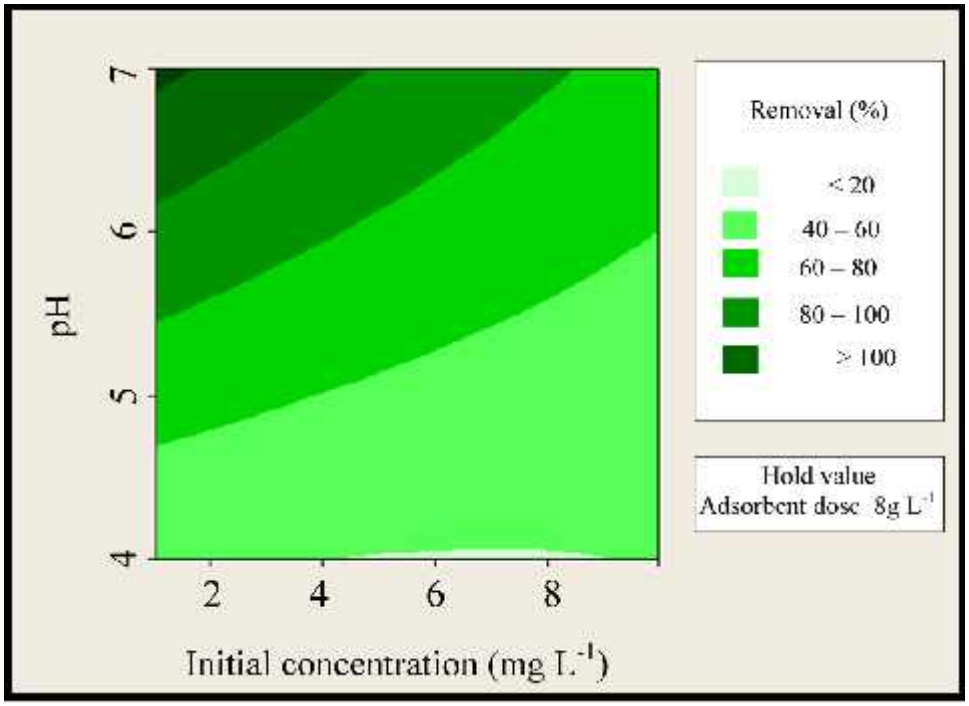

Figure 7.8 Contour plot of 'cadmium removal (%) *vs.* pH and initial concentration (mg L^{-1})' at hold value of adsorbent dose at 8 g L^{-1}

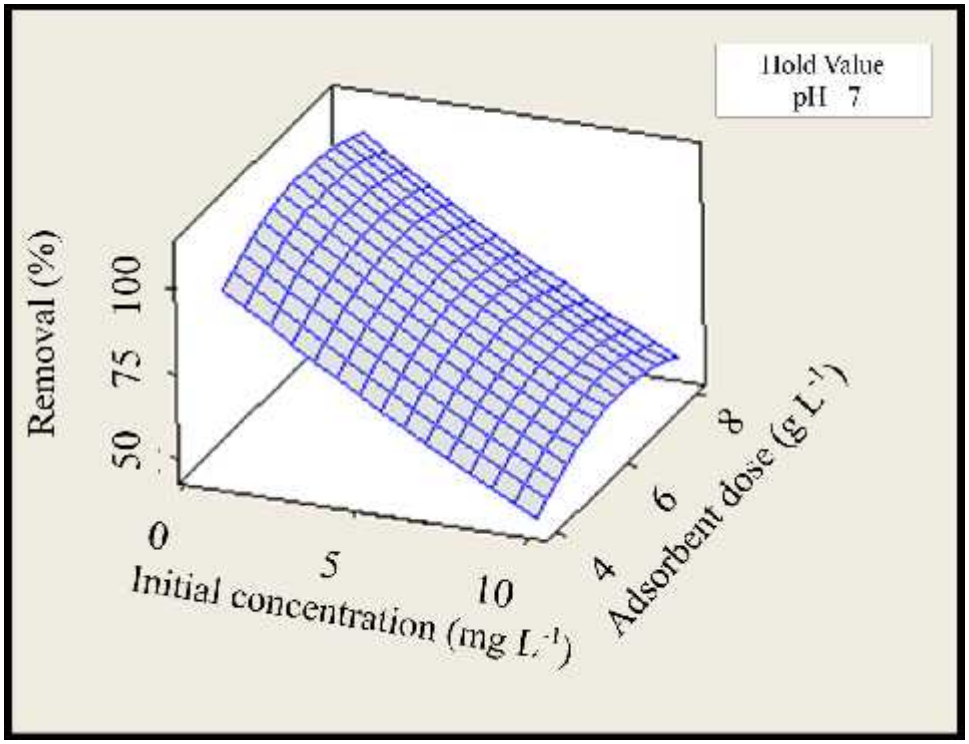

Figure 7.9 Surface plot of 'cadmium removal (%) *vs.* pH and initial concentration (mg L^{-1})' at hold value of pH at 7

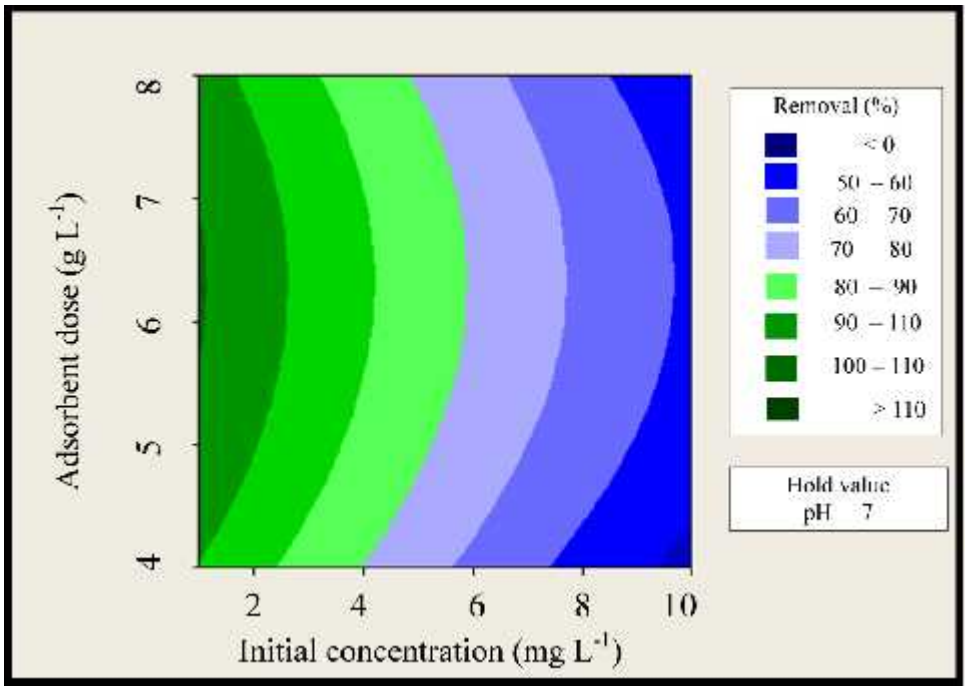

Figure 7.10 Contour plot of 'cadmium removal (%) *vs.* pH and initial concentration (mg L^{-1})' at hold value of pH at 7

7.1.6. Response surface and contour plots

Response surface and contour plot (Figure 7.5 to 7.8) depict that higher cadmium removal (%) was achieved at higher pH (near 7). In the region of pH lower than 6, the cadmium removal was lower than 80 % (Figure 7.6). In plot (Figure 7.10), at initial concentration of more than 6 mg L^{-1}; cadmium removal of less than 80% was predicted. The high cadmium removal (%) is predicted with decreased initial concentration (Figures 7.9 and 7.10). There is minimal difference in slopes of response surface plot (Figure 7.9) between higher initial concentration (10 g L^{-1}) and lower initial concentration (1 g L^{-1}) at variable adsorbent dose. It also depicts minimal change in removal (%) on changing adsorbent dose.

7.1.7. Confirmation experiments

Optimized results suggested by the response surface methodology are as follows: initial concentration =1 mg L^{-1}, initial pH = 6.7, adsorbent dose = 5.2 g L^{-1}. The predicted response was close to experimental results (Table 7.4). However, at pH less than 6 (S.No. 1 in Table 7.4) and in some cases at pH 6 (S.No. 6 and 7 in Table 7.4) experimental results and predicted response show a high degree of difference between them. Hence, the model is valid only at pH greater than 6.

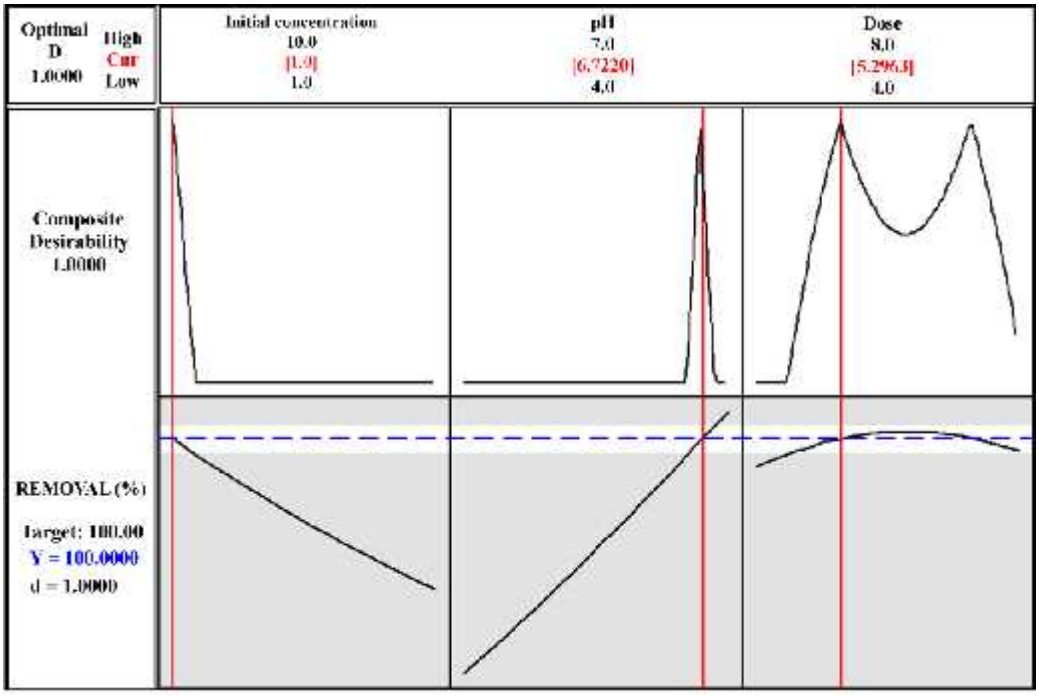

Figure 7.11 Optimisation plot of removal of cadmium from aqueous solution by nano crystalline zirconia

Table 7.4 Confirmation experiments for removal of cadmium using nano crystalline zirconia

S.No.	Initial conc.	pH	Adsorbent dose	Experimental values	Predicted values
1	1	5.5	8	96.62	61.27
2	3	6	6	77.52	71.24
3	3	6.5	8	76.74	78.13
4	4	6.5	4	72.11	67.11
5	4	5.5	4	33.60	43.65
6	4	6	6	45.27	66.80
7	2	6	4	41.20	64.39

The optimized results were further adjusted by varying variables one by one (Table 7.5) and optimized conditions were reached at initial concentration =1, pH = 7 and adsorbent dose = 4 g L^{-1} (Figure 7.11)

Table 7.5 Optimization of removal of cadmium using nano crystalline zirconia

S.No.	Initial conc.	pH	Adsorbent dose	Removal (%)
1	1	7	5.2	100
2	1	7	5	100
3	1	7	4	100
4	1	7	3	99.19
5	1	7	2	97.45
6	2	7	4	85.45
7	3	7	4	75.01
8	4	7	4	75.94
9	5	7	4	51.88

7.2. Linear approach for isotherm analysis

The linear Langmuir isotherm plot (Figure 7.12) showed the predicted data is proximate to experimental data. The linear Freundlich isotherm plot also (Figure 7.13) depicts the proximity of experimental and predicted data. However, one experimental data points or in some cases more than one experimental data points for Freundlich isotherm (Figure 7.13) are far from the predicted data.

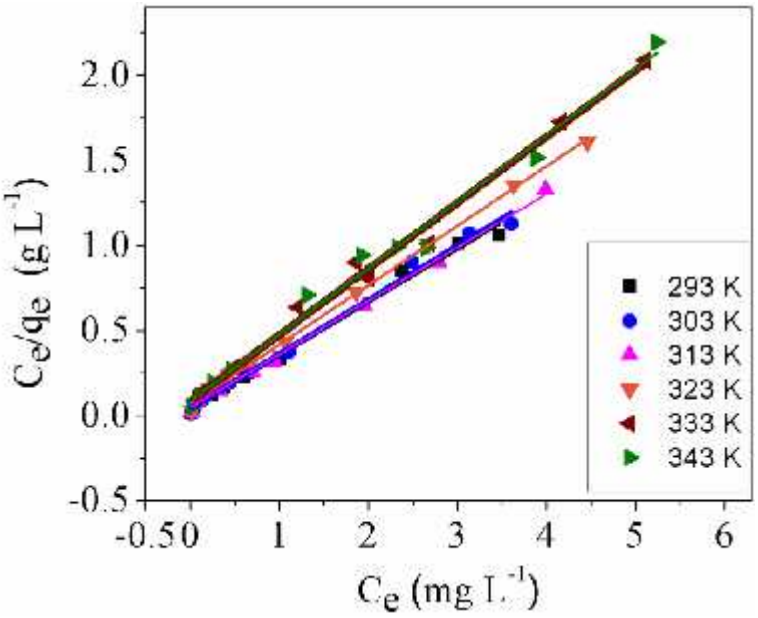

Figure 7.12 Linear Langmuir isotherm plot of cadmium removal using nano crystalline zirconia (dots represent the experimental data and lines represent the data estimated by the model)

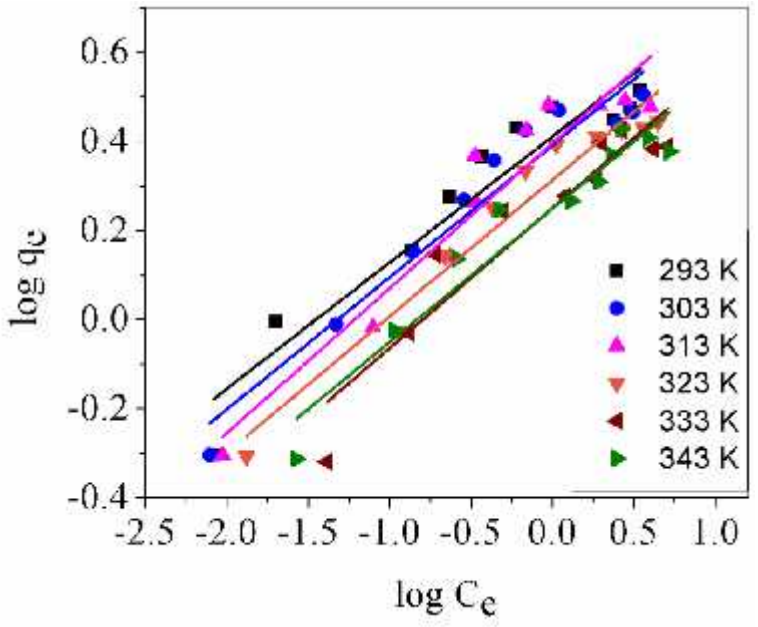

Figure 7.13 Linear Freundlich isotherm plot of cadmium removal using nano crystalline zirconia (dots represent the experimental data and lines represent the data estimated by the model)

Isotherm parameters acquired by linear curve fitting (Figures 7.12 and 7.13) are presented in Table 7.6. The Langmuir isotherm constants i.e. Q_o and b were

calculated from the slopes and intercepts of plot 'C_e/q_e *vs.* C_e'. Langmuir constants Q_o and b were calculated from slope and intercept of fitted curves. The value of Q_o decreased with increase in temperature, pointing to decrease in maximum adsorption capacity with increase of temperature. The Freundlich isotherm parameters K_F and 1/n were calculated from the intercept and slope of plot of 'log q_e *vs.* log C_e'. In Langmuir isotherm model, the values of R^2_{adj} were more than Freundlich isotherm model. So, the linear analysis suggested adsorption of cadmium by nano crystalline zirconia was better fitted in Langmuir isotherm model than Freundlich isotherm model.

Table 7.6 Langmuir and Freundlich isotherm parameters along with coefficient of determination for linear analysis and nonlinear analysis by Microcal origin for adsorption of cadmium from aqueous solution on nano crystalline zirconia

		Langmuir parameters			**Freundlich parameters**		
	Temp.	**Q_o (mg/g)**	**b (L/mg)**	**R^2_{adj}**	**K_F (mg/g)(L/mg)$^{1/n}$**	**1/n**	**R^2_{adj}**
Linear	293	3.1886	8.5315	0.9924	2.5772	0.2833	0.9092
	303	3.1401	7.2536	0.9924	2.4643	0.2968	0.9348
	313	3.1883	6.5321	0.9949	2.4878	0.3258	0.9048
	323	2.8659	5.0195	0.9984	2.0585	0.3064	0.9457
	333	2.5743	4.5241	0.9909	1.7801	0.3150	0.8708
	343	2.5634	4.4623	0.9856	1.7754	0.3003	0.9230
Microcal origin	293	3.1705	7.9353	0.9162	2.5458	0.2170	0.8894
	303	3.1357	6.7191	0.9501	2.4479	0.2273	0.8919
	313	3.3595	4.6345	0.9282	2.4822	0.2419	0.8258
	323	2.8932	4.3329	0.9745	2.0870	0.2425	0.9164
	333	2.5451	4.9455	0.9314	1.8368	0.2433	0.8645
	343	2.5143	4.9436	0.9143	1.8190	0.2441	0.8961

7.3. Nonlinear approach for isotherm analysis

The nonlinear analysis was conducted by error analysis using Microsoft Solver add-in (Figures 7.14 and 7.15) and Microcal origin curve fitting tool (Figures 7.16 and 7.17). The nonlinear Freundlich isotherm plot (Figure 7.14) depicts the vast

difference between the experimental data and data predicted by error analysis method.

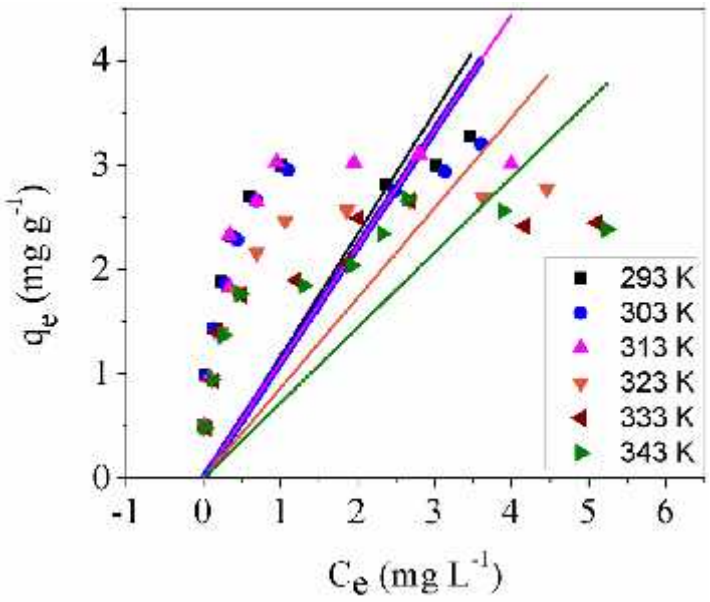

Figure 7.14 Nonlinear Freundlich isotherm plot of cadmium removal using nano crystalline zirconia obtained by error analysis method (dots represent the experimental data and represent the data estimated by the model)

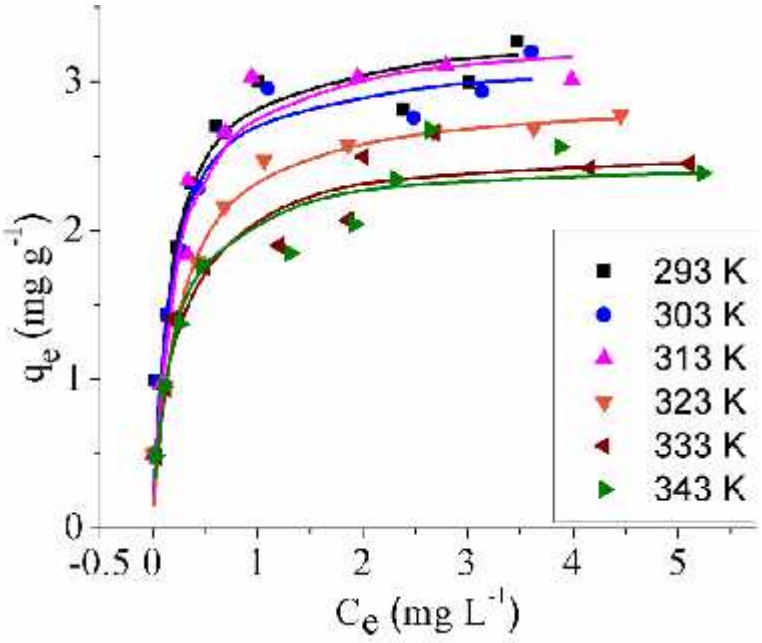

Figure 7.15 Nonlinear Langmuir isotherm plot of cadmium removal using nano crystalline zirconia obtained by error analysis method (dots represent the experimental data and represent the data estimated by the model)

The data predicted by error analysis method depicted in Langmuir isotherm plot (Figure 7.15) is closer to experimental data than in Freundlich isotherm plot (Figure 7.14). However, the data predicted by error analysis method in Langmuir isotherm plot (Figure 7.15) is also less proximate to experimental data. The estimated isotherm parameters by nonlinear analysis are represented in Tables 7.6 and 7.7. In error analysis method, the error function with least normalized sum of error best explains the system (Table 7.7). Marin *et al*. (2007) and Anirudhan et al. (2007) chose HYBRID error function on the basis of least normalized sum of error value for determination of isotherm parameters.In error function analysis of Langmuir isotherm; ARE, ERRSQ, and MPSD explained the three, two and one system respectively better than other error function. In Freundlich isotherm; ERRSQ and HYBRID explains three and two system respectively better than others. The EABS explains one system better than other error function in error function analysis of Freundlich isotherm. In addition to this Freundlich isotherm is selected as best isotherm among chosen with the least normalized sum among two parameters isotherm (Agary *et al.* 2015). Najafi et. al. (2012) apply the high correlation factors and lowest error function to select the sips model by a better fit. On the basis of coefficient of determination; Langmuir isotherm model is more appropriate to be fit onto experimental data (Table 7.7).

Table 7.7 Langmuir and Freundlich isotherm parameters along with coefficient of determination by error analysis method for adsorption of cadmium from aqueous solution on nano crystalline zirconia

	Langmuir parameters				**Freundlich parameters**			
Temp.	**Error function**	**Q_o (mg/g)**	**b (L/mg)**	**R^2_{adj}**	**Error function**	**K_F (mg/g) $(L/mg)^{1/n}$**	**1/n**	**R^2_{adj}**
293 K	ARE	3.3238	6.1596	0.8964	ERRSQ	1.0704	1.0936	-1.7134
303 K	ERRSQ	3.1358	6.7173	0.9042	ERRSQ	1.0389	1.0697	-1.6352
313 K	MPSD	3.3205	5.1380	0.8961	EABS	1.0628	1.0461	-1.8573
323 K	ARE	2.8959	4.2599	0.8946	ERRSQ	0.9318	0.9274	-1.5499
333 K	ERRSQ	2.5451	4.9456	0.9042	HYBRID	0.8804	0.8191	-1.5962
343 K	ARE	2.4627	5.8264	0.8961	HYBRID	0.8804	0.8194	-1.3911

The nonlinear Langmuir isotherm plot (Figure 7.16) depicts the close proximity between the experimental data and data predicted by customized Microcal origin function. The data predicted by customized Microcal origin function depicted in Freundlich isotherm plot (Figure 7.17) is also in proximate position to experimental data. However, experimental data at few locations in Freundlich isotherm plot (Figure

7.17) are far from the predicted data and Langmuir isotherm plot (Figure 7.16) depicts the more close proximity between the experimental data and data predicted by customized Microcal origin function than in Freundlich isotherm plot (Figure 7.17).

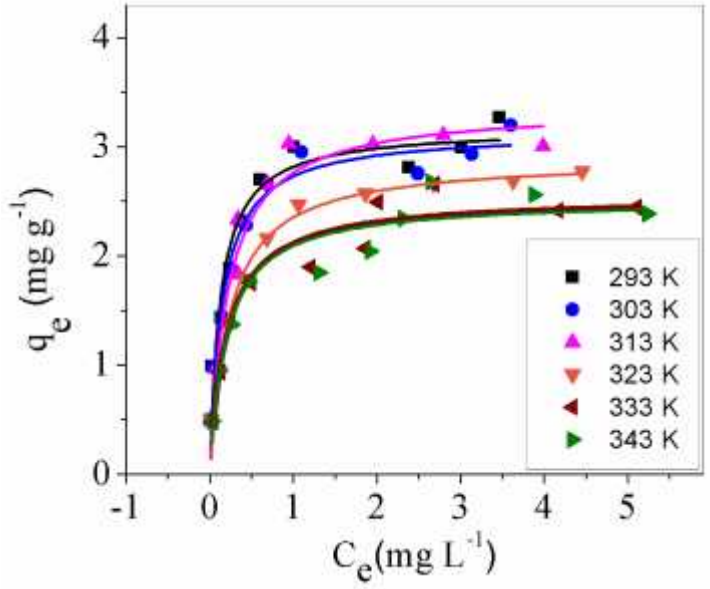

Figure 7.16 Nonlinear Langmuir isotherm plot of cadmium removal using nano crystalline zirconia obtained by customized Microcal origin function (dots represent the experimental data and lines represent the data estimated by the model)

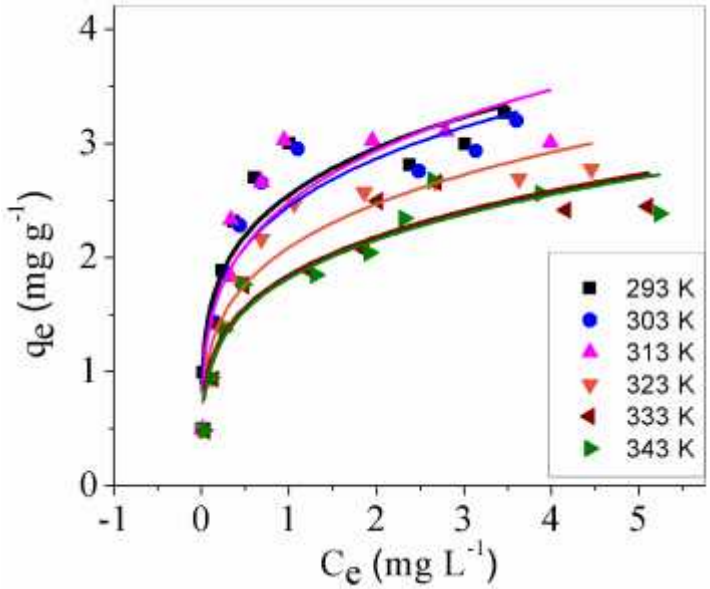

Figure 7.17 Nonlinear Freundlich isotherm plot of cadmium removal using nano crystalline zirconia obtained by customized Microcal origin function (dots represent the experimental data and lines represent the data estimated by the model)

Coefficient of determination using curve fitting function of Microcal origin (Table 7.6) for Langmuir isotherm was better fitted than Freundlich isotherm model.

Hence, the system followed Langmuir isotherm model. The coefficient of determination was appreciative for linear curve fitting analysis than nonlinear curve fitting analysis. So, linear analysis is used to determine isotherm parameters.

7.4. Linear approach for kinetic model analysis

Kinetic parameters estimated from linear (Figures 7.18 and 7.19) and nonlinear curve fitting analysis (Figure 7.20 to 7.23) are presented in Tables 7.8 and 7.9.

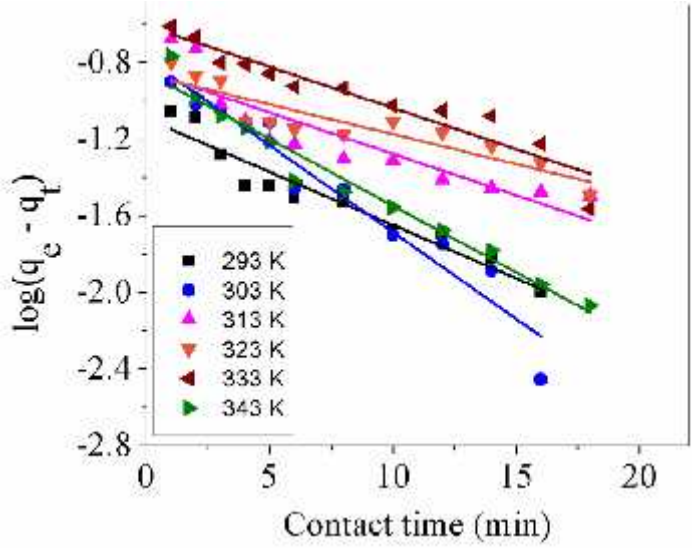

Figure 7.18 Linear pseudo-first order plot of cadmium removal using nano crystalline zirconia (dots represent the experimental data and lines represent the data estimated by the model)

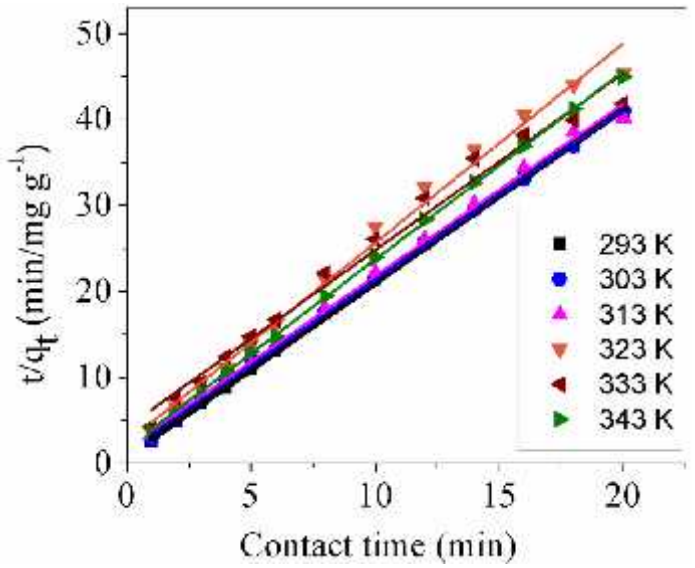

Figure 7.19 Linear pseudo-second order plot of cadmium removal using nano crystalline zirconia (dots represent the experimental data and lines represent the data estimated by the model)

The linear pseudo-first order plot (Figure 7.18) showed the predicted data is less proximate at few experimental data points. The linear pseudo-second order plot (Figure 7.19) depicts the close proximity of experimental and predicted data. The data predicted for pseudo-second order in the plot (Figure 7.19) depicts more proximity of experimental data to predicted data than depicted by pseudo-first order plot (Figure 7.18). Coefficient of determination was higher for pseudo-second order model in contrast to pseudo-first order model (Table 7.8). Experimental q_e values were also more proximate to theoretical values for linear analysis. Pseudo-second order model was found to be more favourable kinetic model on the basis of linear analysis.

Table 7.8 Pseudo-first order and pseudo-second order kinetic parameters for linear analysis and nonlinear analysis by Microcal origin for adsorption of cadmium from aqueous solution on nano crystalline zirconia

			Pseudo-first order			**Pseudo-second order**		
Analysis method	**Temp.**	**Experimental q_e**	**q_e**	**k_1**	**R^2_{adj}**	**q_e**	**k_2**	**R^2_{adj}**
	(K)	**(mg/g)**	**(mg/g)**	**(min^{-1})**		**(mg/g)**	**(g mg^{-1} min^{-1})**	
Linear	293	0.4899	0.0810	0.1234	0.9213	0.4957	4.4833	0.9993
	303	0.4878	0.1666	0.2010	0.9339	0.5044	2.6116	0.9991
	313	0.4983	0.1451	0.0970	0.7806	0.4999	2.2072	0.9971
	323	0.4415	0.1368	0.0711	0.8116	0.4313	2.1790	0.9893
	333	0.4778	0.2491	0.0971	0.8897	0.4856	1.0062	0.9820
	343	0.4445	0.1431	0.1562	0.9659	0.4565	2.6543	0.9995
Microcal origin	293	0.4899	0.4648	1.7580	0.4387	0.4827	8.0832	0.8458
	303	0.4878	0.4554	1.3015	0.4167	0.484	4.5868	0.8098
	313	0.4983	0.4585	0.7240	0.8377	0.4958	2.4478	0.9279
	323	0.4415	0.3807	1.0153	0.4980	0.4072	4.2784	0.7703
	333	0.4778	0.4039	0.5209	0.6657	0.4513	1.6502	0.8516
	343	0.4445	0.4169	0.8669	0.8057	0.4487	3.2459	0.9813

7.5. Nonlinear approach for kinetic model analysis

The nonlinear pseudo-first order plot (Figure 7.20) depicts the close proximity between the experimental data and data predicted by error analysis method. Similarly, nonlinear pseudo-second order plot (Figure 7.21) also depicts the close proximity between the experimental data and data predicted by error analysis

method. The two plots (Figures 7.20 and 7.21) cannot be able to differentiate the suitability of the preferred kinetic model.

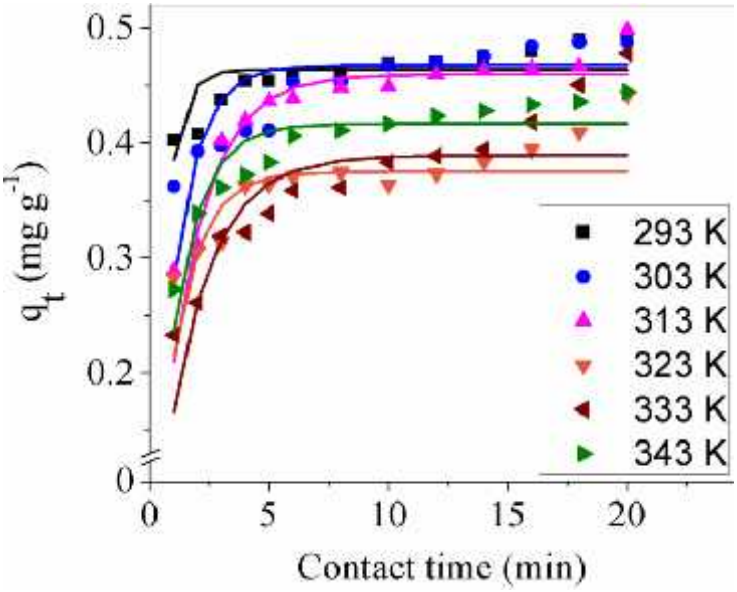

Figure 7.20 Nonlinear pseudo-first order plot of cadmium removal using nano crystalline zirconia obtained by error analysis function (dots represent the experimental data and lines represent the data estimated by the model)

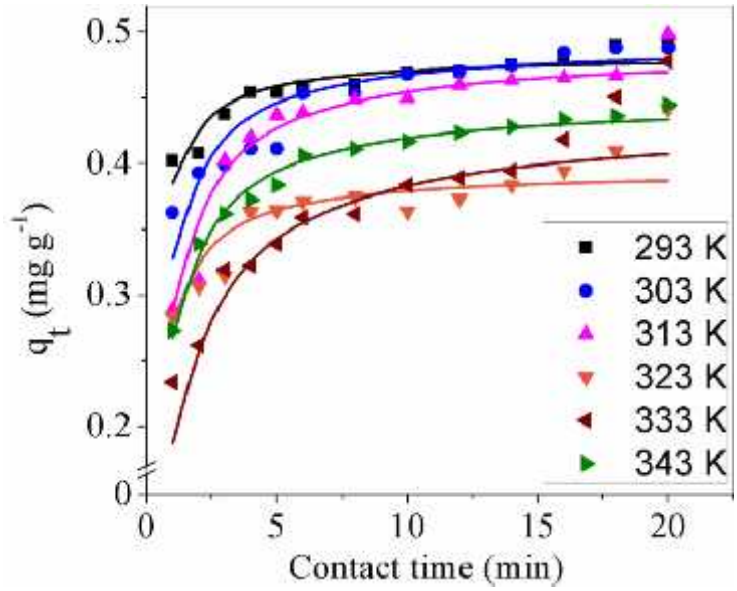

Figure 7.21 Nonlinear pseudo-second order plot of cadmium removal using nano crystalline zirconia obtained by error analysis function (dots represent the experimental data and lines represent the data estimated by the model)

In error analysis method (Figures 7.20 and 7.21) of pseudo-first order model HYBRID, ARE, MPSD and EABS explained one, two, two and one system,

respectively better explained than rest of the error function. In error analysis method of pseudo-second order model two systems each are independently better explained by HYBRID and EABS. ARE and MPSD explains one system each better than other error function. The coefficient of determination is higher for pseudo-first order model (Table 7.9). So, error analysis method suggests the suitability of pseudo-first order model to explain experimental data.

Table 7.9 Pseudo-first order and pseudo-second order model constants by error analysis method for adsorption of cadmium from aqueous solution on nano zirconia

	Pseudo-first order				**Pseudo-second order**			
Temp.		k_1	q_e	R^2_{adj}		k_2	q_e	R^2_{adj}
(K)		**(min^{-1})**	**(mg/g)**			**(g mg^{-1} min^{-1})**	**(mg/g)**	
293	HYBRID	1.7803	0.4638	0.9340	HYBRID	8.2343	0.4822	0.8397
303	MPSD	0.9147	0.4679	0.9994	ARE	4.0619	0.4912	0.7126
313	MPSD	0.6096	0.4600	0.9997	EABS	3.0183	0.4858	0.9092
323	ARE	0.8464	0.3752	0.9996	MPSD	6.1651	0.3947	0.8277
333	EABS	0.5565	0.3894	0.9996	EABS	1.7466	0.4339	0.9041
343	ARE	0.8380	0.4168	0.9998	HYBRID	3.3135	0.4478	0.9825

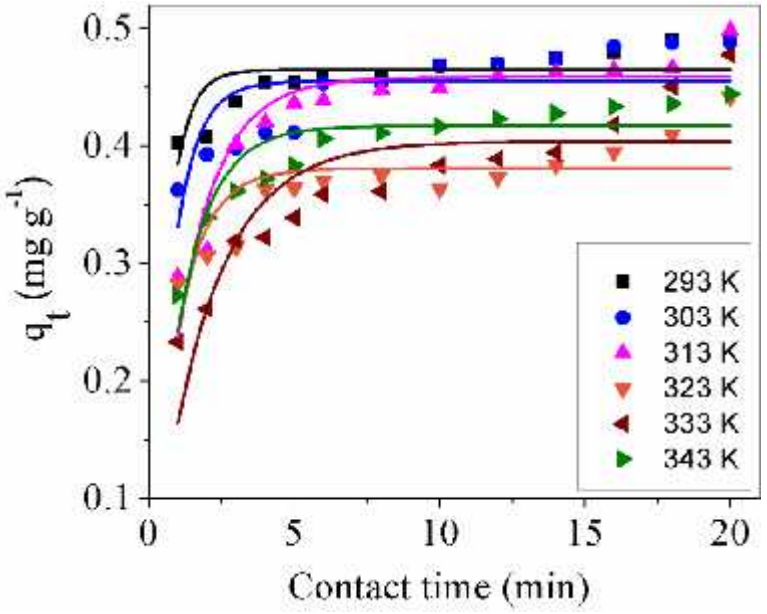

Figure 7.22 Nonlinear pseudo-first order plot of cadmium removal using nano crystalline zirconia obtained by customized Microcal origin function (dots represent the experimental data and lines represent the data estimated by the model)

The nonlinear pseudo-first order plot (Figure 7.22) and pseudo-second order plot (Figure 7.23) showed close proximity of experimental data and data predicted by customized Microcal origin function. The two plots (Figures 7.22 and 7.23) cannot be able to differentiate the suitability of the better model. Nonlinear analysis via Microcal origin (Figures 7.22 and 7.23) suggested pseudo-second order model to be better fitted model than pseudo-first order model on the basis of coefficient of determination (Table 7.8). Linear analysis and nonlinear analysis by Microcal origin advocated the pseudo-second order model to be a better fit model as compared to pseudo-first order model. However, error analysis method suggested the pseudo-first order model to be better fitting model for the present system. The experimental and theoretical q_e values were closer to each other obtained by linear method as compared to error analysis method. So, the system follows pseudo-second order model and linear analysis is preferred due to high coefficient of determination.

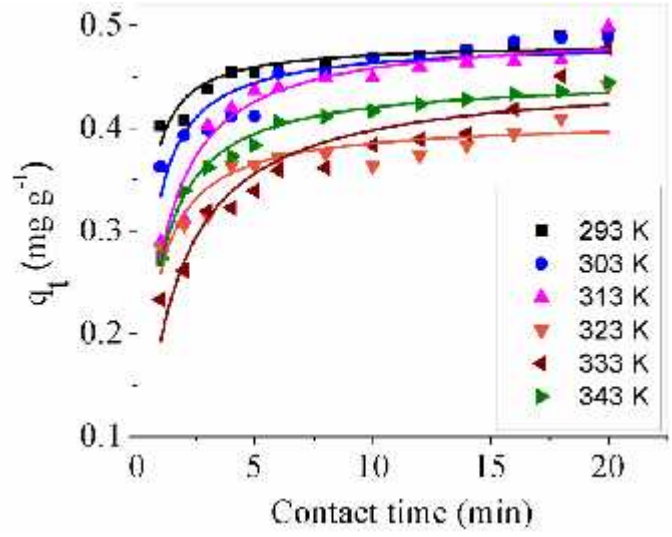

Figure 7.23 Nonlinear pseudo-second order plot of cadmium removal using nano crystalline zirconia obtained by customized Microcal origin function (dots represent the experimental data and lines represent the data estimated by the model)

7.6. Intraparticle diffusion model

The kinetic data was fitted in intraparticle diffusion model suggested by Weber and Morris (Weber and Morris 1963). Intraparticle diffusion graph plotted between q_t and $t^{1/2}$ is shown in Figure 7.24. The K_{diff}, C_b and R^2_{adj} are shown in Table 7.10. The intercept (C_b) depicts the thickness of boundary layer. The bigger

the value of intercept, bigger is the boundary layer. There were two regions in intraparticle diffusion plots. They depict time dependent adsorption process. Initially, the rate of cadmium uptake was faster and afterwards it slowed down with time. The region marked as i and ii symbolize as domination of film diffusion and intraparticle diffusion respectively (Cheung *et al.* 2007).

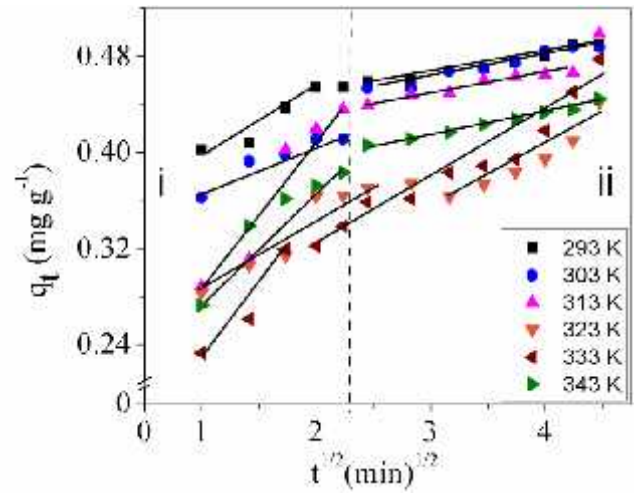

Figure 7.24 Intraparticle diffusion plot for adsorption of cadmium using nanocrystalline zirconia

The intraparticle diffusion plot is not linear and does not pass through the origin. The slope of first and second level shows deviation from origin. The deviation of slope from origin is attributed to the difference in the mass transfer rate of initial and final stages of adsorption. It validates the existence of boundary layer diffusion as rate limiting mechanism for adsorption (Mohanty *et al.* 2005).

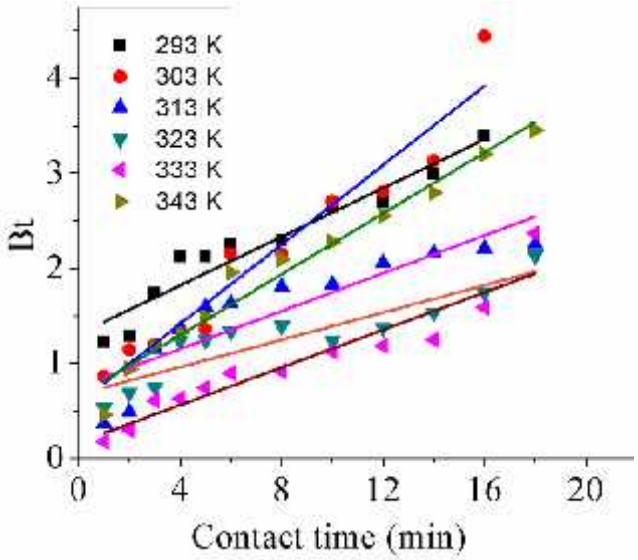

Figure 7.25 Boyd plot for adsorption of cadmium using nanocrystalline zirconia

To further investigate the actual slow step of adsorption process; kinetic data is further analyzed with Boyd model simplified by Reichenberg (Boyd *et al.* 1947;Reichenberg 1953). Boyd model differentiates adsorption rate controlling step between boundary layer and particle diffusion (diffusion inside the pores). Boyd plot is represented by graph (Figure 7.25) between Bt *vs.* t. In the present case, graph (Figure 7.25) did not pass from the origin which means that the process of removal is not controlled by adsorption only, it administrated by boundary layer diffusion mechanism also.

Table 7.10 Intra particle diffusion model parameters for removal of cadmium using nano crystalline zirconia

S.No.	Temperature (K)	K_{diff} (mg/g $min^{1/2}$)	C_b (mg g^{-1})	R^2_{adj}
1	293	0.3919	0.0231	0.8762
2	303	0.3403	0.0362	0.9252
3	313	0.2927	0.0474	0.7380
4	323	0.2653	0.0351	0.8407
5	333	0.1929	0.0599	0.9443
6	343	0.2824	0.0396	0.8301

7.7. Adsorption thermodynamics

7.7.1. Determination of thermodynamic parameters using Langmuir constant method

Thermodynamic parameters i.e. change in standard free energy (ΔG^o), change in standard enthalpy (ΔH^o) and change in standard entropy (ΔS^o) were estimated using subsequent equations (Gupta and Rastogi 2009;Liu 2009;Salvestrini *et al.* 2014):

$$\Delta G_o = -RT\ln K_L \quad (7.3)$$

$$\ln K_L = \frac{\Delta S_o}{R} - \frac{\Delta H_o}{RT} \quad (7.4)$$

The K_L is estimated from the following equation:

$$K_L = \frac{b}{\gamma_e} \tag{7.5}$$

$$\log\gamma_e = -A_1 z^2 I_e^{1/2} \tag{7.6}$$

Here, K_L (L mol^{-1}) is thermodynamic equilibrium constant calculated from the Langmuir constant b (Liu 2009), R is universal gas constant (8.314 J $mol^{-1}K^{-1}$), T is the temperature, γ_e is the activity coefficient, I_e is the ionic strength (3.5 x 10^{-4} mol/ kg) of the solute at equilibrium, A_1 is a constant (0.509 $mol^{-1/2}$ $kg^{1/2}$) and z is the charge on ion. The ΔH^o and ΔS^o were calculated from the slope and intercept of plot between $\ln K_L$ and 1/T respectively (Elkady *et al.* 2011). The calculated values ΔG^o, ΔH^o and ΔS^o parameters are presented in the Table 7.11.

Table 7.11 Thermodynamic parameters estimated by Langmuir constant method for adsorption of cadmium by nano crystalline zirconia

Parameter	**Equation**	**Temp. (K)**	**Parameters using linear equation parameter b**	**Parameters using nonlinear equation parameter b (Microcal origin)**	**Parameters using nonlinear equation parameter b (Excel)**
ΔG^o (kJ mol^{-1})	$\Delta G^o = -RT \ln K_L$	293	-31.8164	-31.6399	-31.0228
		303	-32.4935	-32.3006	-32.3000
		313	-33.2932	-32.4001	-32.6685
		323	-33.6496	-33.2546	-33.2089
		333	-34.4037	-34.6502	-34.6503
		343	-35.3976	-35.6897	-36.1582
ΔH^o (kJ mol^{-1})	$\ln K_L = \frac{\Delta S^o}{R} - \frac{\Delta H^o}{RT}$		-11.805	-8.2816 (-17.242*)	-34.9915 (-10.6645*)
ΔS^o (kJ $mol^{-1}K^{-1}$)			0.06824	0.07874 (0.0492*)	0.09382 (0.07024*)
	Adjusted R^2		0.9513	0.5096 (0.9158*)	0.0304 (0.6234*)

*Excluding data of ln K_L at 333 and 343 K

Thermodynamic parameters were estimated using linear and nonlinear equation parameter b by Langmuir constant method show variation in magnitude. It is estimated that the adsorption process to be spontaneous, exothermic and occurred with increase in entropy.

The thermodynamic equilibrium constant determined by linear analysis method used to calculate thermodynamic parameters. The high R^2_{adj} for linear analysis (0.9543) suggested use of this model.The negative value of enthalpy change (ΔH^o = -11.85 kJ mol^{-1}) advocated the exothermic nature of the adsorption process. The ΔG^o value becomes more negative on raising temperature. It recommends that the feasibility of the process is more at higher temperature. The positive value of entropy change (0.0682 kJ mol^{-1}) suggested the increase of disorderness at adsorbent and adsorbate surface for the adsorption system.

7.7.2. Determination of thermodynamic parameters using partition method

In partition method or distribution coefficient, K_p or K_c is used in place of K_L (Liu 2009;Salvestrini *et al.* 2014):

$$K_P \text{ or } K_C = \frac{C_S}{C_W} \tag{7.7}$$

Here C_s and C_w represent the concentration of adsorbate in solid and liquid phases. Afterwards, the determination of K_c or $K_{p,}$ Equations 7.3 and 7.4 were used for determination of thermodynamic parameters. In addition to this, change in free energy was computed from the following equation (Salvestrini *et al.* 2014):

$$\Delta G_o = \Delta H_o - T\Delta S_o \tag{7.8}$$

The estimation of thermodynamic parameters ΔG^o, ΔH^o and ΔS^o by partitioned method are arranged in Table 7.12. The exothermic nature of adsorption process is estimated by negative value of enthalpy change (ΔH^o = - 70.90 kJ mol^{-1}).Similarly, the values of free energy change (ΔG^o) were negative, recommending that the process is spontaneous in nature. The ΔG^o values calculated from equation 7.8 were also negative, recommending the spontaneous nature of adsorption. The

negative estimation from ΔS^o predicts the decrease of disorderness at adsorbate and adsorbent surface during the process of adsorption. The system is spontaneous in nature and progressed with decline in entropy as evident by aforementioned stated strategy. K_c or K_p is equivalent to thermodynamic equilibrium constant (K_L) only at lower concentration (Liu 2009). So, thermodynamic parameters estimated by Langmuir constant method are preferred over partition method.

Table 7.12 Thermodynamic parameters calculated by partitioned method for adsorption of cadmium by nano crystalline zirconia

Temp. (K)	**ΔG^o (kJ mol^{-1})**	**ΔH^o (kJ mol^{-1})**	**ΔS^o (kJ mol^{-1} K^{-1})**	**R^2_{adj}**	**ΔG^o (kJ mol^{-1})**
	$\Delta G^o = -RT\ln K^p$	$\ln K^p = \frac{\Delta S^0}{R} - \frac{\Delta H^0}{RT}$			$\Delta G^o = \Delta H^o - T\Delta S^o$
293	-9.455	-70.9061	-2.026	0.6267	-115.21
303	-9.291				-94.944
313	-14.782				-74.676
323	-5.425				-54.409
333	-8.496				-34.141
343					-13.873

7.7.3. Activation Energy

Arrhenius equation is used to determine activation energy for adsorption (Arrhenius 1889). The Arrhenius equation is depicted by subsequent equation (Chen *et al.* 2013):

$$\ln k_2 = \ln A - \frac{E_a}{RT} \tag{7.9}$$

Here k_2 (g mg $^{-1}$ min^{-1}) represents the rate constant obtained from the pseudo-second order kinetic model, E_a (J mol^{-1}) is the Arrhenius activation energy of adsorption and A is the Arrhenius factor. The slope of $-E_a/R$ is obtained by a plot between $\ln k_2$ against 1/T. The activation energy calculated is -15.09 kJ mol^{-1}.

7.8. Desorption experiments

Three desorbing agents i.e. hydrochloric acid, nitric acid and sulphuric acid (0.1 N for each solution) solutions were used as desorbing agents for regeneration and

reuse. The HCl, HNO_3 and H_2SO_4 displayed desorption efficiency of 99.25%, 91.75% and 77.25% respectively. HCl solution has shown best results for desorption and the regenerated adsorbent was used up to three cycles successfully for the removal of cadmium (Table 7.13).

Table 7.13 Cadmium removal after subsequent regeneration cycles (Initial concentration = 5 mg L^{-1}, pH = 7, Adsorbent dose = 4 g L^{-1}, Temperature =303 K)

S.No.	Regeneration cycle	Cadmium removal after regeneration cycle (%)
1	1^{st}	69.16
2	2^{nd}	52.48
3	3^{rd}	51.65

7.9. Conclusions

Cadmium was effectively removed from aqueous solutions using nanocrystalline zirconia as an adsorbent. The adsorption equilibrium time was 20 min. The pH was most dominating factor for removal of cadmium using nano crystalline zirconia. The most dominant factor pH was followed by initial concentration and adsorbent dose affecting adsorption of cadmium. Optimum parameters were initial concentration, pH and adsorbent dose at 1 mg L^{-1}, 7 and 4 g L^{-1} respectively. The isotherm and kinetic models data fitted better with linear curve fitting analysis. The data for cadmium removal by nanocrystalline zirconia follows Langmuir isotherm model and pseudo-second order kinetic model. The change in Gibbs free energy was negative showing spontaneous nature of the adsorption process. The adsorption of cadmium using nanocrystalline zirconia was exothermic in nature and occurred with increase of entropy. The regeneration of the adsorbent was done with hydrochloric acid (0.1 N) and showed steady results up to three regeneration cycles.

(Reichenberg 1953)

(Boyd *et al.* 1947)

REFRENCES

Arrhenius, S., Über die Reaktionsgeschwindigkeit bei der Inversion von Rohrzucker durch Säuren, Zeitschrift fuer Physikalische Chemie (Muenchen, Germany),4,226-248,1889.
Boyd, G. E., Adamson, A. W., Myers, L. S., The Exchange Adsorption of Ions from Aqueous Solutions by Organic Zeolites. II. Kinetics1, Journal of the American Chemical Society,69,2836-2848,1947.
Chen, R., Yu, J., Xiao, W., Hierarchically porous MnO2 microspheres with enhanced adsorption performance, Journal of Materials Chemistry A,1,11682-11690,2013.
Cheung, W. H., Szeto, Y. S., McKay, G., Intraparticle diffusion processes during acid dye adsorption onto chitosan, Bioresource Technology,98,2897-2904,2007.
Elkady, M. F., Ibrahim, A. M., El-Latif, M. M. A., Assessment of the adsorption kinetics, equilibrium and thermodynamic for the potential removal of reactive red dye using eggshell biocomposite beads, Desalination,278,412-423,2011.
Gupta, V. K., Rastogi, A., Biosorption of hexavalent chromium by raw and acid-treated green alga Oedogonium hatei from aqueous solutions, Journal of Hazardous Materials,163,396-402,2009.
Liu, Y., Is the Free Energy Change of Adsorption Correctly Calculated?, Journal of Chemical and Engineering Data,54,1981-1985,2009.
Mohanty, K., Das, D., Biswas, M. N., Adsorption of phenol from aqueous solutions using activated carbons prepared from Tectona grandis sawdust by ZnCl2 activation, Chemical Engineering Journal,115,121-131,2005.
Reichenberg, D., Properties of Ion-Exchange Resins in Relation to their Structure. III. Kinetics of Exchange, Journal of the American Chemical Society,75,589-597,1953.
Salvestrini, S., Leone, V., Iovino, P., Canzano, S., Capasso, S., Considerations about the correct evaluation of sorption thermodynamic parameters from equilibrium isotherms, The Journal of chemical thermodynamics,68,310-316,2014.
Wang, F. Y., Wang, H., Ma, J. W., Adsorption of cadmium (II) ions from aqueous solution by a new low-cost adsorbent—Bamboo charcoal, Journal of Hazardous Materials,177,300-306,2010.
Weber, W. J., Morris, J. C., Kinetics of adsorption on carbon from solution, Journal of the Sanitary Engineering Division,89,31-60,1963.